

Heterometallic Ln/Hg Compounds with Fluorinated Thiolate Ligands

Santanu Banerjee, Thomas J. Emge, and John G. Brennan*

Department of Chemistry and Chemical Biology, Rutgers, the State University of New Jersey, 610 Taylor Road, Piscataway, New Jersey 08854-8087

Received June 16, 2004

The early lanthanide benzenefluorothiolates ($\text{Ln}(\text{SC}_6\text{F}_5)_3$; Ln = La, Ce, Pr, Nd, Sm, Gd) react with $\text{Hg}(\text{SC}_6\text{F}_5)_2$ in DME to form ionic heterometallic compounds with Ln cations and Hg anions. X-ray diffraction analyses of all compounds reveal an isostructural series with the general formula $[(\text{DME})_3\text{Ln}(\text{SC}_6\text{F}_5)_2]_2[\text{Hg}_2(\text{SC}_6\text{F}_5)_6]$. In the structures, a fluorothiolate ligand has been extracted from the Ln coordination sphere that is saturated with three neutral DME donor ligands and a dative interaction between one ortho fluorine and the Ln. Distances between Ln and F do not vary simply with Ln ionic radius. There are two Ln cations with charge balanced by a $\text{Hg}_2(\text{SC}_6\text{F}_5)_6$ dianion composed of two distinctly nonideal Hg(II) tetrahedra, all connected through a series of π - π interactions that link cations with anions in a one-dimensional array and anions to anions in a more complex 2D network.

Introduction

Heterometallic compounds containing lanthanides (Ln) and transition metals (M) continue to be investigated as potentially useful electronic materials with readily tailored electronic or magnetic properties.^{1–6} There is an extensive litera-

ture describing the use of pseudohalide ligands (CN ,² SCN ,³ SPh ,⁴ SePh^5) to connect Ln with M, and a recent description of a LnHg compound with an iodide linkage.⁶ Within this molecular class, both charge neutral and ionic species have been prepared. The more conventional ionic ligands tend to maintain Ln–L connectivity, whereas ligands that preferentially form more covalent bonds are often expelled from Ln coordination spheres, giving rise to ionic species with solvated Ln.

Lanthanide compounds with certain pseudohalogen ligands will react with elemental chalcogen, reducing the chalcogen and oxidizing the pseudohalide, to form chalcogenido clusters.⁷ This redox reactivity roughly parallels that of the ligand displacement chemistry. More covalent ligands (i.e., SPh, SePh, TePh) are readily abstracted from Ln, and they react with elemental E, reducing E to give E^{2-} with concomitant oxidation of L^- to give L–L . In contrast, the more ionic ligands remain coordinated to Ln and do not react with elemental E (i.e., halogens). Finally, there are ligands with intermediate reactivity patterns, i.e., CN, SCN, and the halides, which can be extracted from Ln coordination spheres but do not appear to reduce elemental E. An extension of this chemistry to heterometallic systems led to the preparation of selenido cluster salts, with separate cationic Ln_4Se and anionic M_4Se cluster cores.^{7a}

Fluorinated benzenethiolate (SC_6F_5) is a particularly interesting ligand for lanthanide compounds, because the fluor-

* To whom correspondence should be addressed. E-mail: bren@rutchem.rutgers.edu.

- (1) (a) Imbert, D.; Cantuel, M.; Buenzli, J.; Bernardinelli, G.; Piguat, C. *J. Am. Chem. Soc.* **2003**, *125*, 15698–15699. (b) Rodriguez-Cortinas, R.; Avecilla, F.; Platas-Iglesias, C.; Imbert, D.; Buenzli, J.; de Blas, A.; Rodriguez-Blas, T. *Inorg. Chem.* **2002**, *41*, 5336–5349. (c) Buenzli, J. G.; Piguat, C. *Chem. Rev.* **2002**, *102*, 1897–1928. (d) Glover, P. B.; Ashton, P. R.; Childs, L. J.; Rodger, A.; Kercher, M.; Williams, R. M.; De Cola, L.; Pikramenou, Z. *J. Am. Chem. Soc.* **2003**, *125*, 9918–9919. (e) Lin, X.; Doble, D. M. J.; Blake, A. J.; Harrison, A.; Wilson, C.; Schroeder, M. *J. Am. Chem. Soc.* **2003**, *125*, 9476–9483. (f) He, Z.; He, C.; Gao, E.; Wang, Z.; Yang, X.; Liao, C.; Yan, C. *Inorg. Chem.* **2003**, *42*, 2206–2208. (g) Cui, Y.; Qian, Y.-T.; Huang, J.-S. *Polyhedron* **2001**, *20*, 1795–1802.
- (2) (a) James, C.; Willand, P. S. *J. Am. Chem. Soc.* **1916**, *38*, 1497. (b) Bailey, W. E.; Williams, R. J.; Milligan, W. O. *Acta Crystallogr.* **1973**, *B29*, 1365. (c) Knoepfel, D. W.; Liu, J.; Meyers, E. A.; Shore, S. G. *Inorg. Chem.* **1998**, *37*, 4828–4837. (d) Liu, J.; Knoepfel, D. W.; Liu, S.; Meyers, E. A.; Shore, S. G. *Inorg. Chem.* **2001**, *40*, 2842–2850. (e) Du, B.; Meyers, E. A.; Shore, S. G. *Inorg. Chem.* **2001**, *40*, 4353–4360. (f) James, C.; Willand, P. S. *J. Am. Chem. Soc.* **1916**, *38*, 1497. (g) Harada, K.; Yuzunihara, J.; Ishii, Y.; Sato, N.; Kambayashi, H.; Fukada, Y. *Chem. Lett.* **1995**, 887.
- (3) Amirkhanov, V. M.; Kapshuk, A. A.; Kramarenko, F. G.; Skopenko, V. V. *Russ. J. Inorg. Chem.* **1994**, *39*, 1155.
- (4) Brewer, M.; Emge, T.; Brennan, J. *Inorg. Chem.* **1995**, *34*, 5919–24.
- (5) (a) Freedman, D.; Emge, T. J.; Brennan, J. G. *J. Am. Chem. Soc.* **1997**, *119*, 11112–3. (b) Lee, J.; Emge, T.; Brennan, J. *Inorg. Chem.* **1997**, *36*, 5064–8. (c) Berardini, M.; Emge, T.; Brennan, J. *Inorg. Chem.* **1995**, *34*, 5327. (d) Berardini, M.; Emge, T.; Brennan, J. *J. Am. Chem. Soc.* **1994**, *116*, 6941.
- (6) Huebner, L.; Emge, T. J.; Brennan, J. G. *Inorg. Chem.* **2004**, *43*, 5659–5664.

- (7) (a) Kornienko, A.; Huebner, L.; Freedman, D.; Emge, T.; Brennan, J. *Inorg. Chem.* **2003**, *42*, 8476–80.

inated organic ring imparts useful solubility properties. For example, (solvent)₆Ln₄E(EE)₄(SC₆F₅)₂ dissolve readily in toluene,⁸ whereas (solvent)₆Ln₄E(EE)₄(EPh)₂ (E = S, Se, Te) are soluble only in Lewis base solvents. The fluorocarbon moiety also imparts curious structural features, including extensive π - π stacking interactions,⁹ and in lanthanide chemistry there exists a distinct tendency to exhibit dative Ln-F interactions.¹⁰ In redox reactions of Ln(SC₆F₅)₃ with elemental E, the fluorothiolate ligand did not react, thus presenting an opportunity to prepare the aforementioned toluene soluble clusters.

While displacement chemistry (or the lack thereof) with SC₆F₅ has been examined, heterometallic Ln compounds incorporating SC₆F₅ have not yet been described. Because hydrocarbon soluble heterometallic compounds could be useful for doping Ln/M into a variety of organic based optoelectronic devices, we set out to establish whether Ln(SC₆F₅)₃ would react with Hg(SC₆F₅)₂ to form discrete products. This work outlines the first successful preparation of heterometallic fluorothiolate compounds containing both Ln and Hg, the first structural characterization of heterometallic compounds containing SC₆F₅ ligands, and the first attempt to evaluate how Ln ionic radius influences the length of dative Ln-F bonds.

Experimental Section

General Methods. All syntheses were carried out under high purity nitrogen (Airgas), using conventional drybox or Schlenk techniques. Solvents (Aldrich) were either refluxed continuously over molten alkali metals or K/benzophenone and collected immediately prior to use, or purified with a dual column Solv-Tek solvent purification system. Lanthanides were purchased from Strem. Hg(SC₆F₅)₂ was prepared according to the modified^{10a} literature procedure.¹¹ Melting points were taken in sealed capillaries and are uncorrected. IR spectra were taken on a Thermo Nicolet Avatar 360 FTIR spectrometer, and recorded from 4000 to 600 cm⁻¹ as a Nujol mull on NaCl plates. Mass spectra were recorded on a Finnigan LCQ-DUO mass spectrometer using acetonitrile as a solvent. Electronic spectra were recorded on a Varian DMS 100S spectrometer with the samples in a 0.10 mm quartz cell attached to a Teflon stopcock. Elemental analyses were performed by Quantitative Technologies, Inc. (Whitehouse NJ). The compounds are slightly air sensitive and will eventually lose lattice DME when exposed to air.

Synthesis of [(DME)₃La(SC₆F₅)₂]₂[Hg₂(μ -SC₆F₅)₂(SC₆F₅)₄]₂·2DME (1). Method A follows: La (0.14 g, 1.0 mmol) and Hg(SC₆F₅)₂ (1.50 g, 2.5 mmol) were combined in DME (ca. 20 mL), and the mixture was stirred until all the metal was consumed (1 day) to give a colorless solution with black powdery precipitate

at the bottom of the flask. The colorless solution was filtered away and reduced in volume under vacuum to ca. 10 mL and layered with hexane (10 mL) to give colorless plate-shaped crystals on cooling at 15 °C (0.30 g, 88%) that melt between 75 and 80 °C, turn light yellow at 100 °C, darken between 170 and 175 °C, and remain dark brown from 200 to 350 °C. IR: 2950 (w), 2920 (w), 2856 (w), 2407 (s), 2343 (s), 1631 (s), 1456 (m), 1374 (m), 1345 (m), 1299 (m), 1252 (m), 1077 (s), 1001 (s), 960 (s), 709 (s) cm⁻¹. UV-vis.: no absorption maximum from 300 to 750 nm when dissolved in either THF or pyridine. Anal. Calcd for C₉₂H₈₀F₅₀Hg₂O₁₆S₁₀La₂: C, 32.6; H, 2.36. Found: C, 32.2; H, 2.50. ¹⁹F NMR (CD₃CN, 24 °C): -162.57 (1F, w_{1/2} = 90 Hz); -161.68 (2F, w_{1/2} = 136 Hz); -130.95 (2F, w_{1/2} = 90 Hz). There was no change in line shape as a function of temperature. Method B follows: La (0.14 g, 1.0 mmol) and Hg(SC₆F₅)₂ (0.90 g, 1.5 mmol) were combined in DME (ca. 20 mL), and the mixture was stirred overnight until all the metal was consumed with the appearance of elemental mercury at the bottom of the flask. The colorless solution was filtered away from the mercury (0.25 g, 82%), and Hg(SC₆F₅)₂ (0.60 g, 1.0 mmol) was added to the solution and stirred overnight to give a colorless solution with a gray powdery precipitate at the bottom of the flask. The colorless solution was filtered, reduced in volume under vacuum (10 mL), and layered with 10 mL of hexane to give colorless plate-shaped crystals upon cooling at 15 °C (0.30 g, 88%).

Synthesis of [(DME)₃Ce(SC₆F₅)₂]₂[Hg₂(μ -SC₆F₅)₂(SC₆F₅)₄]₂·2DME (2). As for **1** above, Ce (0.14 g, 1.0 mmol) and Hg(SC₆F₅)₂ (1.50 g, 2.5 mmol) in DME (ca. 20 mL) gave colorless small rod shaped crystals (0.28 g, 82%). The crystals melt (colorless liquid) between 80 and 82 °C; the liquid then turns pale yellow at 120 °C, and then dark brown around 220 °C. IR: 2925 (w), 2725 (s), 2593 (s), 2396 (s), 2351 (s), 1622 (m), 1575 (s), 1463 (w), 1385 (w), 1296 (m), 1261 (w), 1085 (w), 970 (w), 857 (w), 712 (s), 622 (s) cm⁻¹. UV-vis.: no absorption maximum from 300 to 750 nm in either THF or pyridine. Anal. Calcd for C₉₂H₈₀F₅₀Hg₂O₁₆S₁₀Ce₂: C, 32.5; H, 2.36. Found: C, 32.0; H, 2.22. ¹⁹F NMR (CD₃CN, 24 °C): -162.69 (1F, w_{1/2} = 91 Hz); -161.56 (2F, w_{1/2} = 136 Hz); -131.2 (2F, w_{1/2} = 90 Hz). There was no change in line shape as a function of temperature. Method B follows: As for **1** above, Ce (0.14 g, 1.0 mmol) and sequential additions of Hg(SC₆F₅)₂ (0.90 g, 1.5 mmol and 0.60 g, 1 mmol) in DME (ca. 20 mL) produced colorless small rod-shaped crystals (0.28 g, 82%).

Synthesis of [(DME)₃Pr(SC₆F₅)₂]₂[Hg₂(μ -SC₆F₅)₂(SC₆F₅)₄]₂·2DME (3). As for **1** above, Pr (0.14 g, 1.0 mmol) and Hg(SC₆F₅)₂ (1.50 g, 2.5 mmol) in DME (ca. 20 mL) gave pale green plate-shaped crystals (0.33 g, 97%) that melt between 72 and 75 °C. The liquid turns deeper green at 140 °C and changes from light brown to dark brown between 245 and 350 °C. IR: 2926 (w), 2729 (w), 2397 (s), 2255 (s), 1711 (s), 1659 (s), 1622 (s), 1579 (w), 1456 (w), 1386 (w), 1257 (w), 1089 (w), 824 (w), 721 (m), 623 (s) cm⁻¹. UV-vis.: no absorption maximum from 300 to 750 nm in either THF or pyridine. Anal. Calcd for C₉₂H₈₀F₅₀Hg₂O₁₆S₁₀Pr₂: C, 32.5; H, 2.35. Found: C, 31.7; H, 2.19. ¹⁹F NMR (CD₃CN, 24 °C): -162.79 (1F, w_{1/2} = 136 Hz); -161.22 (2F, w_{1/2} = 136 Hz); -131.45 (2F, w_{1/2} = 272 Hz). There was no change in line shape as a function of temperature. Method B follows: As for **1**, Pr (0.14 g, 1.0 mmol) and sequential additions of Hg(SC₆F₅)₂ (0.90 g, 1.5 mmol and 0.60 g, 1 mmol) in DME (ca. 20 mL) gave pale green crystals (0.33 g, 97%).

Synthesis of [(DME)₃Nd(SC₆F₅)₂]₂[Hg₂(μ -SC₆F₅)₂(SC₆F₅)₄]₂·2DME (4). As for **1**, Nd (0.14 g, 1.0 mmol) and Hg(SC₆F₅)₂ (1.50 g, 2.5 mmol) in DME (ca. 20 mL) gave, upon cooling to 5 °C, colorless crystals (0.27 g, 79%) that melt between 70 and 74 °C.

(8) Fitzgerald, M.; Emge, T. J.; Brennan, J. G. *Inorg. Chem.* **2002**, *41*, 3528-43.

(9) (a) Anderson, K. M.; Baylies, C. J.; Monowar-Jahan, A. H. M.; Norman, N. C.; Orpen, A. G.; Starbuck, J. *Dalton Trans.* **2003**, 3270-3277. (b) Crespo, O.; Canales, F.; Gimeno, M. C.; Jones, P. G.; Laguna, A. *Organometallics* **1999**, *18*, 3142-3148. (c) Uson, M. A.; Llanos, J. M. *J. Organomet. Chem.* **2002**, *663*, 98-107. (d) Carmalt, C. J.; Dinnage, C. W.; Parkin, I. P.; White, A. J. P.; Williams, D. J. *Dalton* **2000**, 3500-3504. (e) Chadwick, S.; English, U.; Noll, B.; Ruhlandt-Senge, K. *Inorg. Chem.* **1998**, *37*, 4718-4725.

(10) (a) Melman, J.; Rhode, C.; Emge, T. J.; Brennan, J. G. *Inorg. Chem.* **2002**, *41*, 28-33. (b) Melman, J.; Emge, T. J.; Brennan, J. G. *Inorg. Chem.* **2001**, *40*, 1078-81.

(11) Peach, M. E. *J. Inorg. Nucl. Chem.* **1973**, *35*, 1046.

Table 1. Summary of Crystallographic Details for 1–6

	1	2	3	4	5	6
Ln in empirical formula	La	Ce	Pr	Nd	Sm	Gd
$C_{92}H_{80}F_{50}Hg_2O_{16}S_{10}Ln_2$						
fw	3391.16	3393.58	3395.16	3401.82	3414.04	3427.84
space group	$P\bar{1}$	$P\bar{1}$	$P\bar{1}$	$P\bar{1}$	$P\bar{1}$	$P\bar{1}$
a (Å)	12.6352(7)	12.6701(7)	12.6591(6)	12.6488(7)	12.6489(10)	12.6757(6)
b (Å)	13.1976(7)	13.2133(7)	13.1702(7)	13.2025(7)	13.1545(11)	13.1765(6)
c (Å)	19.6962(10)	19.6719(11)	19.5725(10)	19.5108(10)	19.4412(16)	19.4107(9)
α (deg)	87.021(1)	87.041(1)	87.046(1)	87.149(1)	87.170(2)	87.270(1)
β (deg)	83.928(1)	84.001(1)	84.107(1)	84.017(1)	83.838(2)	83.758(1)
γ (deg)	63.923(1)	63.974(1)	64.036(1)	64.092(1)	64.053(1)	64.065(1)
V (Å ³)	2933.5(3)	2943.1(3)	2918.2(3)	2914.8(3)	2891.9(4)	2898.2(2)
Z	1	1	1	1	1	1
D (calcd) (g/cm ⁻³)	1.920	1.915	1.932	1.938	1.960	1.964
T (°C)	-173	-173	-173	-173	-173	-173
λ (Å)	0.71073	0.71073	0.71073	0.71073	0.71073	0.71073
abs coeff (mm ⁻¹)	3.638	3.674	3.674	3.819	3.967	4.090
$R(F)^a$ [$I > 2 \sigma(I)$]	0.046	0.055	0.039	0.069	0.057	0.044
$R_w(F^2)^a$ [$I > 2 \sigma(I)$]	0.096	0.113	0.091	0.114	0.131	0.102

^a Definitions: $R(F) = \sum ||F_o| - |F_c|| / \sum |F_o|$; $R_w(F^2) = \{\sum [w(F_o^2 - F_c^2)^2] / \sum [w(F_o^2)^2]\}^{1/2}$. Additional crystallographic details are given in the Supporting Information.

The liquid turns light yellow at around 160 °C and dark brown between 230 and 350 °C. IR: 2918 (w), 2722 (w), 2395 (m), 2360 (m), 2249 (s), 2208 (s), 2022 (s), 1975 (s), 1934 (s), 1712 (s), 1655 (s), 1619 (m), 1564 (s), 1456 (w), 1327 (w), 1251 (w), 1187 (w), 861 (w), 726 (w), 616 (s) cm⁻¹. UV-vis: no absorption maximum from 300 to 750 nm in either THF or pyridine. Anal. Calcd for $C_{92}H_{80}F_{50}Hg_2O_{16}S_{10}Nd_2$: C, 32.5; H, 2.35. Found: C, 31.6; H, 2.19. ¹⁹F NMR (CD₃CN, 24 °C): -162.52 (1F, $w_{1/2}$ = 210 Hz); -160.5 (2F, $w_{1/2}$ = 210 Hz); -131.32 (2F, $w_{1/2}$ = 210 Hz). There was no change in line shape as a function of temperature. Method B follows: As for **1** above, Nd (0.14 g, 1.0 mmol) and sequential addition of Hg(SC₆F₅)₂ (0.90 g, 1.5 mmol and 0.60 g, 1.0 mmol) in DME (ca. 20 mL) gave colorless crystals upon cooling at 15 °C (0.27 g, 79%). Thermal decomposition: **4** was placed in a quartz tube sealed under vacuum. The end charged with the compound was placed in a tube furnace while the other end was immersed in liquid nitrogen. The temperature was ramped to 700 °C at a rate of 20°/min, and then held for 3 h. Analysis of the residual solid-state material with a Bruker D8 Advance XRP diffractometer identified NdF₃ as the only crystalline solid-state product present.¹²

Synthesis of [(DME)₃Sm(SC₆F₅)₂]₂[Hg₂(μ -SC₆F₅)₂(SC₆F₅)₄]₂DME (5**).** Method A follows: As for **1**, Sm (0.15 g, 1.0 mmol) and Hg(SC₆F₅)₂ (1.50 g, 2.5 mmol) in DME (ca. 20 mL) gave light yellow plate-shaped crystals on cooling at 15 °C (0.29 g, 84%). The compound melts between 72 and 75 °C, turns yellow at 140 °C, and changes from light brown to dark brown between 245 and 350 °C. IR: 2926 (w), 2729 (w), 2397 (s), 2255 (s), 1711 (s), 1659 (s), 1622 (s), 1579 (w), 1456 (w), 1386 (w), 1257 (w), 1089 (w), 824 (w), 721 (m), 623 (s) cm⁻¹. UV-vis: no absorption maximum from 300 to 750 nm in either THF or pyridine. Anal. Calcd for $C_{92}H_{80}F_{50}Hg_2O_{16}S_{10}Sm_2$: C, 32.3; H, 2.34. Found: C, 32.1; H, 2.00. ¹⁹F NMR (CD₃CN, 24 °C): -162.84 (1F, $w_{1/2}$ = 141 Hz); -161.42 (2F, $w_{1/2}$ = 140 Hz); -131.61 (2F, $w_{1/2}$ = 98 Hz). There was no change in line shape as a function of temperature. Method B follows: As for **1**, Sm (0.15 g, 1.0 mmol) and sequential additions of Hg(SC₆F₅)₂ (0.90 g, 1.5 mmol and 0.60 g, 1 mmol) in DME (ca. 20 mL) gave light yellow plate-shaped crystals (0.29 g, 84%).

Synthesis of [(DME)₃Gd(SC₆F₅)₂]₂[Hg₂(μ -SC₆F₅)₂(SC₆F₅)₄]₂DME (6**).** As for **1**, Gd (0.157 g, 1.0 mmol) and Hg(SC₆F₅)₂ (1.50 g, 2.5 mmol) in DME (ca. 20 mL) gave colorless small rodlike crystals (0.28 g, 82%) which melt (colorless liquid) between 65 and 70 °C. The liquid turns pale yellow at 160 °C and continues to a dark brown color between 230 and 350 °C. IR: 2922 (w), 2725

(m), 2391 (s), 2251 (s), 1706 (s), 1657 (s), 1625 (s), 1577 (s), 1462 (w), 1363 (w), 1258 (w), 1088 (w), 1018 (w), 865 (m), 804 (m), 722 (m) cm⁻¹. UV-vis: no absorption maximum from 300 to 750 nm in either THF or pyridine. Anal. Calcd for $C_{92}H_{80}F_{50}Hg_2O_{16}S_{10}Gd_2$: C, 32.2; H, 2.33. Found: C, 31.5; H, 2.46. ¹⁹F NMR (CD₃CN, 24 °C): -162.77 (1F, $w_{1/2}$ = 101 Hz); -161.22 (2F, $w_{1/2}$ = 105 Hz); -131.45 (2F, $w_{1/2}$ = 196 Hz). There was no change in line shape as a function of temperature. Method B follows: As for **1** above, Gd (0.16 g, 1.0 mmol) and sequential addition of Hg(SC₆F₅)₂ (0.90 g, 1.5 mmol and 0.60 g, 1.0 mmol) in DME (ca. 20 mL) gave colorless crystals upon cooling at 15 °C (0.28 g, 82%).

X-ray Structure Determination of 1–6. Data for **1–6** were collected on a Bruker Smart APEX CCD diffractometer with graphite monochromatized Mo K α radiation (λ = 0.71073 Å) at 100 K. The data were corrected for Lorentz effects and polarization, and absorption, the latter by a multiscan (SADABS)¹³ method. The structures were solved by Patterson or direct methods (SHELXS86).¹⁴ All non-hydrogen atoms were refined (SHELXL97)¹⁵ on the basis of F_{obs}^2 . All hydrogen atom coordinates were calculated with idealized geometries (SHELXL97). Scattering factors (f_o , f' , f'') are as described in SHELXL97. Crystallographic data and final R indices for **1–6** are given in Table 1. A generic ORTEP diagram¹⁶ for **1–6** is shown in Figure 1. Significant bond geometries for **1–6** are given in Table 2. Complete crystallographic details for **1–6** are given in the Supporting Information.

Results

Lanthanide benzenefluorothiolates (Ln(SC₆F₅)₃; Ln = La, Ce, Pr, Nd, Sm, Gd) react with mercury benzenefluorothiolate to form ionic heterometallic compounds with the general formula [(DME)₃Ln(SC₆F₅)₂]₂[Hg₂(SC₆F₅)₆] (Ln = La (**1**), Ce (**2**), Pr (**3**), Nd (**4**), Sm (**5**), Gd (**6**)). These

(12) Staritzky, E.; Asprey, L. B. *Anal. Chem.* **1957**, *29*, 856–7.

(13) SADABS, Bruker Nonius area detector scaling and absorption correction, v2.05; Bruker-AXS Inc.: Madison, WI, 2003.

(14) Sheldrick, G. M. *SHELXS86, Program for the Solution of Crystal Structures*; University of Göttingen: Göttingen, Germany, 1986.

(15) Sheldrick, G. M. *SHELXL97, Program for Crystal Structure Refinement*; University of Göttingen: Göttingen, Germany, 1997.

(16) (a) Johnson, C. K. *ORTEP II*; Report ORNL-5138; Oak Ridge National Laboratory: Oak Ridge, TN, 1976. (b) Zsolnai, L. *XPMA and ZORTEP, Programs for Interactive ORTEP Drawings*; University of Heidelberg: Heidelberg, Germany, 1997.

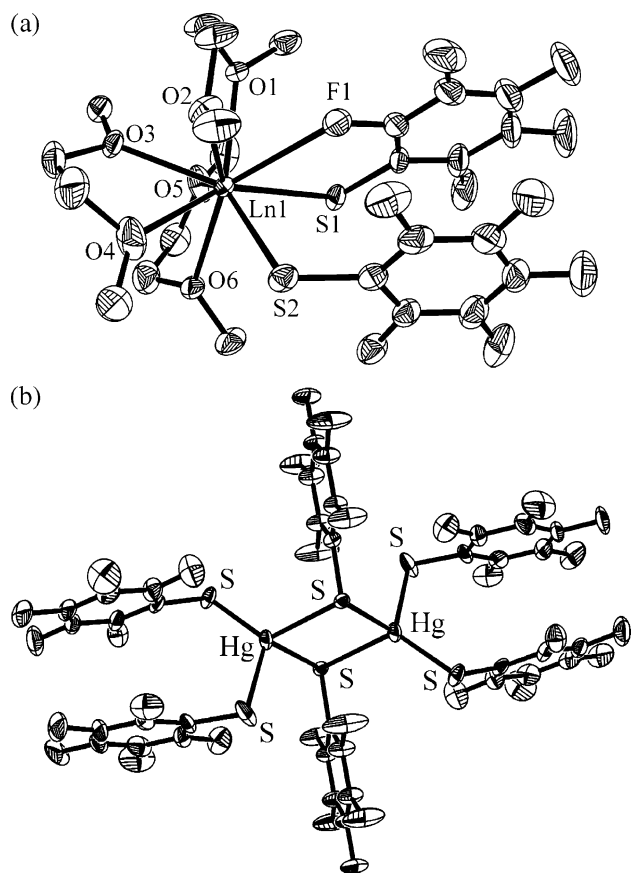
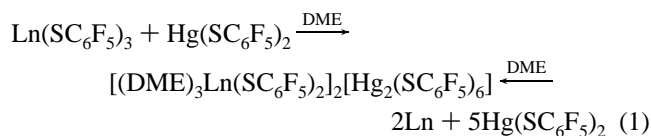


Figure 1. Molecular structure of the cation (a) and dianion (b) in $[(\text{DME})_3\text{Ln}(\text{SC}_6\text{F}_5)_2]_2[\text{Hg}_2(\text{SC}_6\text{F}_5)_4(\mu_2\text{-SC}_6\text{F}_5)_2]$. Thermal ellipsoids are drawn at the 50% probability level for the Pr compound.

compounds can be prepared either by combining solutions of Ln and Hg reagents or by in situ generation of the Ln reagent in the presence of excess $\text{Hg}(\text{SC}_6\text{F}_5)_2$ (reaction 1). They are insoluble in apolar solvents (i.e., hexane, toluene) but redissolve in Lewis bases such as pyridine, acetonitrile, or THF. Once isolated, they are relatively stable in air and can be handled briefly with no immediate loss of crystallinity. Attempts to prepare the analogous Eu(III) derivative led only to the isolation of divalent $[\text{Eu}(\text{SC}_6\text{F}_5)_2]_n$,^{10a} and the later (heavier) lanthanides do not appear to form isolable compounds.



Low-temperature single-crystal X-ray diffraction analyses of **1–6** were obtained, revealing an isostructural series of solvated Ln cations with mercury dianions. Figure 1 gives an ORTEP diagram for the Pr derivative as a generic structure of **1–6**, and Table 2 gives a listing of significant bond lengths and angles in the complexes. In all compounds, the Ln ions are each chelated by three bidentate DME ligands distributed on one side of the metal. There are two terminal thiolates on the other side, one of which also coordinates to the Ln through a dative bond to the ortho fluoride F(1). The Ln–S and Ln–O bond lengths vary with Ln ionic radius,

with the lanthanide contraction accounting for the decrease upon traversing the series from La to Gd (Table 2). In contrast, Ln–F bonds vary in a discontinuous fashion: there is at first a statistically equal set of distances noted from La to Ce to Nd, before a small but steady increase in Ln–F(1) bond length from Nd to Sm, and finally a more dramatic increase at Gd. Pure compounds with lanthanides heavier than Gd were not obtained.

Both cations and anions have intermolecular π – π interactions for adjacent pairs of SC_6F_5 ligands that generate an anion that is flattened on two sides. For the cations, this placement of ligands results in a rather polar molecular species, in contrast to the anion, which contains near inversion symmetry. The flattened molecular shape lends itself to low-dimensional stacking of ions in the crystal structure. For the $[(\text{DME})_3\text{Ln}(\text{SC}_6\text{F}_5)_2]_2[\text{Hg}_2(\text{SC}_6\text{F}_5)_4]$ salts, as in other molecular salts, this also gives rise to segregated 2D sheets of cations that alternate with sheets of anions in the solid state. Further, the anions form infinite chains of directly overlapping pairs of SC_6F_5 ligands between adjacent ions. These chains criss-cross along the crystallographic *a* and *b* directions for the inversion-related pairs of SC_6F_5 ligands in the anion to yield a tightly woven 2D sheet of closely interacting anions. Although the *a* and *b* axes differ significantly in length, there is no crystallographic distinction between pairs of terminal SC_6F_5 ligands of the anion, since inversion symmetry is imposed on the anion by the space group. As a result, the geometry of the intermolecular π – π interactions along the *a* versus *b* directions is approximately the same. This situation accommodates the 50:50 disorder for two sites for each of these terminal SC_6F_5 ligands in the anion, in contrast to the ordered cation. The packing motif for the cations leads to an ordered, but lower dimensional, stacking array, as the cations pair up to form discrete dimers with one intramolecular and two intermolecular π – π interactions. The one DME solvate molecule per Ln is found in the cation sheet, filling a void between cation pairs at the interface to the anion sheet.

Discussion

While the SC_6F_5 moiety has, until now, provided an entry into hydrocarbon soluble molecular and cluster chemistry of the lanthanides, compounds **1–6** are soluble only in Lewis base solvents. Molecular Ln(II) and Ln(III) compounds¹⁰ routinely dissolved in aromatic solvents such as toluene, and even the chalcogen rich $(\text{THF})_6\text{LnE}(\text{EE})_4(\text{SC}_6\text{F}_5)_2$ clusters,⁸ which had only two SC_6F_5 ligands to solubilize four Ln centers, were toluene soluble. Presumably, the unusual insolubilities of **1–6** originate from the ionic nature of the products. Previously, 1D structures had been noted, i.e., $\text{Eu}(\text{SC}_6\text{F}_5)_2$,^{10a} where pairs of bridging thiolates connected adjacent Eu ions and π – π interactions connecting neighboring sets of SC_6F_5 ligands. Even though $\text{Eu}(\text{SC}_6\text{F}_5)_2$ formed a polymeric lattice, the compound itself dissolved in apolar solvents. Compounds **1–6**, with 2D sheets of anions isolating the layers of Ln containing cations, represent the first set of Ln compounds with SC_6F_5 ligands that are totally insoluble in hydrocarbon solvents. The large molecular dipole of the

Table 2. Significant Distances (Å) and Angles (deg) for **1–6**

	La	Ce	Pr	Nd	Sm	Gd
Ln(1)–O(2)	2.563(3)	2.547(3)	2.528(2)	2.512(4)	2.475(4)	2.459(3)
Ln(1)–O(6)	2.578(2)	2.548(3)	2.536(2)	2.524(4)	2.486(4)	2.465(3)
Ln(1)–O(4)	2.617(3)	2.590(4)	2.552(3)	2.545(5)	2.496(5)	2.483(3)
Ln(1)–O(1)	2.586(2)	2.570(3)	2.546(2)	2.526(4)	2.496(4)	2.480(3)
Ln(1)–O(3)	2.601(2)	2.598(3)	2.569(2)	2.554(5)	2.535(4)	2.515(3)
Ln(1)–O(5)	2.640(3)	2.626(3)	2.604(3)	2.592(5)	2.562(4)	2.554(3)
Ln(1)–F(1)	2.797(2)	2.811(3)	2.799(2)	2.801(4)	2.813(3)	2.837(3)
Ln(1)–S(2)	2.8935(10)	2.8692(12)	2.8431(8)	2.8316(18)	2.8011(15)	2.7909(10)
Ln(1)–S(1)	2.9277(9)	2.9034(11)	2.8807(8)	2.8656(17)	2.8307(14)	2.8171(10)
Ln–S(1)–C(1)	108.1(1)	108.3(2)	108.7(1)	108.5(3)	109.1(2)	109.9(2)
Ln–S(2)–C(7)	110.1(1)	111.4(2)	112.1(1)	112.5(2)	113.2(2)	114.0(1)

Ln containing cations must also play a role in the insolubility of **1–6**.

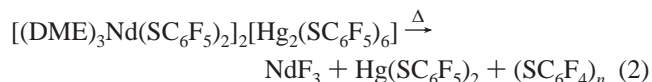
Still, solid-state structure is not necessarily identical to solution structure. ^{19}F NMR analyses in THF and acetonitrile give some information regarding structure in solution. In acetonitrile, the compounds show only a single set of ortho, meta, and para F resonances, suggesting either that the solution state contains only a single type of SC_6F_5 environment, or that there is fast site exchange that averages the inequivalent mercury bonding environments (terminal and bridging) with those of the terminal and chelating lanthanide thiolates. In THF, the La compound again shows only a single resonance for the meta and para fluorides, but the ortho resonance is split 3:1, which suggests that there are distinct Ln versus Hg containing molecular ions in THF solution, and that site exchange between Ln and Hg thiolates is slow on the NMR time scale. The molecular form of the anions is not defined by the NMR experiment, but the tendency of $\text{Hg}_2(\text{SR})_6^{2-}$ to convert to $\text{Hg}(\text{SR})_3^-$ in neutral donor solvents is well-known.¹⁷ Mass spectra for the La and Pr compounds in acetonitrile were obtained, and the negative ion spectra contained a series of identifiable peaks, including SC_6F_5 ($M^- = 199.6$), $\text{Hg}(\text{SC}_6\text{F}_5)_3^-$ ($M^- = 798.7$), $(\text{CH}_3\text{CN})\text{Hg}(\text{SC}_6\text{F}_5)_3^-$ ($M^- = 837.2$), and $\text{Hg}_2(\text{SC}_6\text{F}_5)_5^-$ ($M^- = 1393.9$), with relative intensities of 1:20:7:14. Clearly, the structure in solution is more complicated than that in the solid state.

Previous studies have shown that elemental S will displace SPh but not SC_6F_5 from lanthanide coordination spheres $\text{Ln}(\text{ER})_3$, which implies that $\text{Ln}-\text{S}(\text{C}_6\text{F}_5)$ bonds are chemically more robust than are $\text{Ln}-\text{S}(\text{Ph})$ bonds in redox reactions.⁷ This, coupled with earlier work that found no absolute evidence for Hg(II) promoted abstraction of SPh from Ln coordination spheres, led to the mistaken assumption that $\text{LnHg}(\text{SC}_6\text{F}_5)_x$ compounds would also adopt molecular, rather than ionic, structures.

Clearly, a number of factors are influencing these differences in reactivity. Presumably, the different strengths of the formed disulfide linkages are important in the redox work, but solvent effects are also both possible and intangible in the heterometallic chemistry, given that parallel experiments with SPh and SC_6F_5 did not yield interpretable results. Heterometallic syntheses with SPh ligands in THF always produced insoluble, essentially intractable products at room temperature and pressure, and only with Eu(II) could a

discrete heterometallic thiolate, namely $[(\text{py})_3\text{EuHg}(\text{SPh})_4]_2$, be isolated by dissolving the product in a stronger Lewis base.⁴ Unfortunately, with the SC_6F_5 ligand a crystalline heterometallic product was obtained only from DME. Still, the fact that both heterometallic SPh and SC_6F_5 compounds are so dramatically less soluble than their monometallic components suggests that SPh ligands are also being abstracted from Ln.

One distinct difference in the chemistry of heterometallic SPh and SC_6F_5 compounds is noted in a thermolysis experiment. While $\text{Ln}(\text{C}_6\text{F}_5)_3$ compounds have already been shown to decompose thermally to give LnF_3 ,¹⁰ it was unclear whether the ionic configurations of **1–6** would have any impact on the identity of the thermolysis products, and so an analysis of the thermal decomposition of **4** was undertaken. In contrast to the thermolysis of heterometallic Ln/Hg SPh compounds,⁴ which gave mixtures of LnS and HgS, decomposition of **4** gave only solid-state NdF_3 , with the mercury fluorothiolate subliming into the cold zone of the thermolysis experiment prior to decomposition (reaction 2).



The mercury dianion is distinctly distorted from ideal tetrahedral Hg(II) geometries. Although the inner Hg_2S_2 cores are crystallographically required to be planar (which still allows for tetrahedral symmetry), the bridging ligands show no evidence of disorder, the average $\text{S}-\text{Hg}-\text{S}'$ angles and average $\text{Hg}-\text{S}-\text{Hg}'$ angles are within a degree of 90° and sum to approximately 180° for **1–6**. This distortion from tetrahedral geometry (i.e., 109.5° angles) and planarity is observed also in the related $\text{Hg}_2(\text{SPh})_6^{2-}$ (89.5° and 90.5° , respectively, for $\text{S}-\text{Hg}-\text{S}$ and $\text{Hg}-\text{S}-\text{Hg}$),¹⁸ even though the latter compound does not display significant inter- or intramolecular $\pi-\pi$ interactions between SPh ligands. A related anion, $\text{Hg}_2(\text{SMe})_6^{2-}$, contains a mercury–sulfur core that also has Hg geometries that are far from tetrahedral ($\text{S}-\text{Hg}-\text{S}$, 94.2°).¹⁹ Disorder within the dianion in **1–6** complicates an analysis of the Hg–S bond lengths beyond the above, but all refined to values within the normal range of Hg–S interactions.

(18) Bowmaker, G. A.; Dance, I. G.; Harris, R. K.; Henderson, W.; Laban, I.; Scudder, M. L.; Oh, S.-W. *J. Chem. Soc., Dalton Trans.* **1996**, 2381.

(19) Bowmaker, G. A.; Dance, I. G.; Dobson, B. C.; Rogers, D. A. *Aust. J. Chem.* **1984**, *37*, 1607.

(17) Henkel, G.; Krebs, B. *Chem. Rev.* **2004**, *104*, 801–24

Within a given cation, interplanar distances increase slightly on going from the more interior contacts, at 3.2 Å, and for the more exterior contacts, at 3.8 Å. This increase in contact distances is consistent with the inflexibility associated with the bidentate [e.g., S(1)–Ln–F(1)] ligand and the flexibility of the adjacent monodentate [e.g., S(2)–Ln] ligand. Within the anions, the dihedral angle between adjacent terminal C₆F₅ rings is also not zero. However, the contact distances decrease on going from the more interior 3.6 Å contacts to the more exterior 3.2 Å contacts. This decrease in contact distances is consistent with the type of nontetrahedral disorder observed for the Hg coordination. These distances, 3.6 Å on the interior and 3.2 Å on the exterior, are observed for the entire series here, **1–6**. As for intermolecular ring–ring contacts, there are none for the isolated cations, but the disorder in the terminal ligands of the anion allows for two sets of contact distances between parallel rings that are crystallographically equivalent, namely, A···B and B···A. For all anions in complexes **1–6**, the intermolecular separation between nearest neighbor rings is parallel at a 3.5 Å separation. This is expected for closely stacking rings that are related by a symmetry center, as found in the 2D array of anions here.

Finally, this isostructural series presents a unique opportunity to evaluate the manner by which steric demands impact dative Ln–F bond lengths. From the distances in Table 2, it becomes clear that these Ln–F interactions are influenced by more than just the ionic radii of Ln and F. The six Ln–O and two Ln–S bonds all behave as expected, gradually contracting as the size of Ln decreases with the lanthanide contraction.²⁰ This gradual decrease serves to increase interligand repulsive interactions, and the bond most sensitive to these repulsions is Ln–F, the weakest bond within the primary Ln coordination sphere. In the early compounds **1–3**, there are no significant differences in Ln–F

bond lengths, which range from La–F (2.797(2) Å) to Nd–F (2.801(4) Å) and are compared to distances noted, for example, in [(THF)₃Ce(SC₆F₅)₃]₂ (2.749(2) Å) and (py)₄Sm(SC₆F₅)₃ (2.703(5) Å).^{10b} As the series progresses, there is a small but constant increase in the distance separating Ln and F. With Ln ionic radii decreasing from **1** to **6** (La = 1.30 Å; Gd = 1.19 Å),²⁰ the increase in Ln–F separation from Nd (2.801(4) Å) to Gd (2.837(3) Å) must be originating from interligand repulsive interactions that increase as the entire Ln coordination sphere contracts.

Support for this steric interpretation is found in the series of Ln–S–C angles, which increase as the series progresses from La to Gd (see Table 2). The nonchelating S(2) ligand is affected more, with Ln–S(2)–C(7) increasing from 110.1(1)° (La) to 114.0(1)° (Gd). In the chelating thiolate, this opening of Ln–S(1)–C(1) is significant only for Gd, much as was found in the series of Ln–F distances. The inability to isolate compounds with Ln smaller than Gd could be resulting from a change in molecular conformation as the Ln–F interaction becomes unsustainable.

Conclusion

Lanthanide and mercury benzenefluorothiolates react to form stable, relatively insoluble heterometallic compounds with transfer of thiolate from Ln to Hg. This anion transfer persists in solution. Contributing to the stability of the observed solid-state structure is an extensive network of π – π interactions that connect anions with both cations and neighboring anions. The dative Ln–F bond lengths in the structures do not vary with Ln ionic radius.

Acknowledgment. This work was supported by the National Science Foundation under Grant CHE-0303075.

Supporting Information Available: X-ray crystallographic files in CIF format for the crystal structures of **1–6**. This material is available free of charge via the Internet at <http://pubs.acs.org>.

(20) Shannon, R. D. *Acta Crystallogr., Sect. A* **1976**, *32*, 751.